A study of recent improvements in spallation reaction models

S E Taylor
CEA/Saclay, F-91191, Gif-Sur-Yvette Cedex, France

Abstract

New developments in the combined Liege intra-nuclear cascade and ABLA evaporation model for studying spallation reactions have been investigated. Predictions of proton, neutron and Helium-4 cross-sections have been made for nucleons incident on a variety of targets at a range of incident energies, and these have been compared to those obtained using previous versions of the model. The recent modifications are found to have had a beneficial effect on the predictions of the model for the most part, particularly for Helium-4 cross-sections, which were previously only accommodated in the evaporation part of the model. However, in some cases the modifications seem to have had a detrimental effect on predictions of some observables, particularly for neutron double-differential cross sections on lead at low incident energies. Taken as a whole, the results are encouraging, but also indicative of some small flaws that future improvements will need to address.

1 Introduction

Spallation reactions are of interest in a number of different fields, not least nuclear waste management [1], radioactive beam production [2] and even astrophysics [3]. The last 10 years or so have seen great advances made in the development of both theoretical and experimental tools for the study of spallation reactions for such applications. New, powerful spallation sources - for example SNS in the USA and J-PARC in Japan - helped to drive interest in spallation reactions, but optimising the spallation sources of facilities like these can be difficult empirically given the large number of parameters that characterise these sources, creating a need for particle transport codes that can be used to study spallation reactions. One such code is the INCL-ABLA model, which couples the INCL high-energy intra-nuclear cascade model to the ABLA low-energy evaporation model in a two-step process common to studying reactions of this type.

These codes, and others in the same vein, are generally good at describing neutron production from proton or neutron induced reactions in heavy targets. However, light charged particle (e.g. helium, deuteron, tritium) production was until recently either very poorly predicted, or not included in the model at all, as was the case for tritium (see, for example, [4, 5] for more information). Given that a build up of helium within a spallation reactor can cause damage to the window and/or structural materials [6], and that tritium, a beta emitter

with a 12 year half life, can contribute significantly to the target radioactivity, the relatively poor modelling of light charged particle production in spallation reactions was a major shortcoming of the INCL-ABLA model. However, recent steps have been taken to rectify this problem, and new versions of INCL and ABLA (INCL4.5 and ABLA07) have been released as a result. This paper provides a systematic study of the new version of the INCL-ABLA model by comparing its output to that obtained with a previous version (INCL4.2 + ABLA version KHSv3p) for a number of different observables, to identify the wide-ranging ramifications of the recent modifications. Please note that the calculation results for the new versions of INCL and ABLA, the experimental data files and the tools for building the figures displayed in this report were all downloaded from the IAEA 'Benchmark of Spallation Models' online resource [7].

2 The Numerical model

2.1 The INCL intra-nuclear cascade model

INCL is a time-like intra-nuclear cascade (INC) model, which follows the fate of all particles in space-time and contains a self-consistent stopping criterion (a feature unique to INCL). More details of INCL can be found at [8], but the main ingredients of the model are as follows:
The nucleons are initially positioned within the target according to a Saxon-Woods distribution [9] of the form:

$$\rho(r) = \frac{\rho_0}{1 + exp\left(\frac{r-R_0}{a}\right)} \tag{1}$$

for $r < R_{max}$, with $\rho(r)$ equal to zero elsewhere. ρ_0 is a normalisation constant, a determines the diffuseness of the nuclear surface and R_0 is a measure of the nuclear size. For our purposes, R_{max} is taken to be $R_0 + 8a$. The momentum distribution of the nucleons is taken as a Fermi sphere with Fermi momentum p_F. Note, however, that the greater momentum a nucleon has, the farther out from the center of the nucleus it is able to travel, and thus the distributions governing the position $\vec{r}$ and the momentum $\vec{p}$ cannot be taken independently. Rather, nucleons of momentum $\vec{p}$ are placed in a square well of depth V_0, with a momentum dependent radius of $R(p)$. Then, the initial positions and momentums of the nucleons are generated by taking $\vec{p}$ at random in a sphere of radius p_F and using this to calculate $R(p)$ from the following equation:

$$\left(\frac{p}{p_F}\right)^3 = -\frac{4\pi}{3A_T}\int_0^{R(p)} \frac{d\rho(r)}{dr} r^3 dr. \tag{2}$$

$\vec{r}$ is then chosen at random in a sphere of radius $R(p)$ [8]. This approach is necessary in INCL since the particles are propagated in single steps between avatars, during which time their momenta should be free to change.

Upon initialisation of the simulation, particles are forced to travel in straight lines until either two of them collide, one is transmitted or reflected at the nuclear surface, or a delta resonance decays. These occurances are referred to as avatars. Three types of particles are considered in INCL: nucleons, Δ-isobars

and pions. The incident particles are nucleons in all cases for this study, although INCL can also accomodate deuteron, tritium, ^{3}He, ^{4}He and pion incident particles. Each time a particle is emitted its type, kinetic energy and direction are recorded. The mass number, excitation energy, recoil energy, direction, charge and angular momentum of the remnant nucleus are also recorded. This recorded information is then passed to the evaporation model.

INCL also includes a novel determination of the stopping time of the simulation, based on studies [5] of the time variation of the average values of many physical quantities calculated during the simulation. The stopping time is given by:

$$t_{stop} = f_{stop} t_0 \left(\frac{A_T}{208} \right)^{0.16}, \tag{3}$$

with $t_0 = 70$fm/c and f_{stop} a free parameter, usually taken as 1. Note this stopping time is independent of the energy and impact parameter of the incident projectile.

The main modifications incorporated in the latest version of INCL (4.5) are as follows (more details can be found in [8]):

1. Light charged particle (LCP) emission has been included in INCL4.5 (see 'Cluster Emission' section below for a description of how this has been implemented).

2. The nucleon potential has been modified to be isospin and kinetic energy dependent. The potential is still modelled as a square well with a momentum dependent radius, but now inside this radius the total energy (E) is equal to:

$$E = \frac{\hbar^2 k^2}{2M} + V(\tau, T), \tag{4}$$

   where $V(\tau, T)$ is a function of the isospin τ and the kinetic energy T. Outside the momentum dependant radius the potential is still assumed to be zero. Detailed information on the modifications to the nucleon potential can be found in [10].

3. An average potential for pions is included in INCL4.5. See [11] for more details, but it is worth pointing out that although pion production is not studied in this work, this modification is expected to have a (minor) effect on the calculation of other observables as well.

4. In INCL4.5 events are either terminated at t_{stop}, as before, *or* when all particles have energies less than the Fermi Energy plus 10 MeV. Note, this modification is not expected to change the numerical results, rather it was introduced as it reduces the computational time needed by around 25%.

Cluster Emission

Light charged particle emission in INCL4.5 is dealt with in the following way:

1. When a nucleon is emitted at the nuclear surface, it is allowed to drag other nucleons with it that are sufficiently close in phase space, and thus form a cluster. The clusters considered in INCL4.5 are d, t, ^{3}He, ^{4}He and any other clusters up to $A = 8$ (although for this work only ^{4}He was studied).

2. Of the possible clusters that can be formed, the one with the lowest excitation energy is emitted *providing* its total energy (kinetic energy plus potential energy minus binding energy) is positive *and* it manages to tunnel through the Coulomb barrier. If either of these tests are failed, only the leading nucleon is emitted (provided it manages to tunnel through the Coulomb barrier).

Finally, it should be pointed out that INCL is, in essence, a parameter free code, since the parameters set by hand in the code are only included for cluster production and their values are severely restricted by phenomenolgical concerns. The other main variable, f_{stop} (as described earlier), was given its standard value (unity) for this study, and regardless other work [5] has shown changing its value around this (within reason) does not drastically affect results.

2.2 The ABLA evaporation model

ABLA07 is a time-like Monte-Carlo dynamical code for describing the de-excitation of a thermal system. Full details of the model can be found elsewhere [12], but three main mechanisms for de-excitation are considered. First, particle emission from the thermalised nucleus is calculated following the Weisskopf-Ewing formalism [13], with the emissions of protons, gamma rays, light charged particles with Z =1–2 and intermediate mass fragments (IMF) with $Z > 2$ all considered. The standard Weisskopf-Ewing approach is extended to include the change in angular momentum due to particle emission.
Second, fission of the nucleus, when applicable, is dealt with by the PROFI model [14, 15], with only binary fission considered.
Finally, the excited system can undergo simultaneous break-up via the cracking of the nucleus into several fragments (induced by thermal fluctuations) [16], and this is explicitly treated by the model.

For comparison, the previous version of the ABLA code, the Schmidt evaporation model version KHSv3p (henceforth called v3p), was also studied. A description of this code can be found in Refs. [17, 18]. For clarity, the main differences between the two models are given below:

1. ABLA07 uses an extended Weisskopf-Ewing formalisation for calculating particle emission, which includes angular momentum considerations. v3p uses the standard Weisskopf-Ewing formalism, which does not.

2. Only the emission of neutrons, protons and ^{4}He is considered in v3p, whereas ABLA07 also includes the emission of other LCP and IMF (as described earlier), and takes gamma rays into account when calculating emission candidates. Note that for this work only the emission of nucleons and ^{4}He were studied.

3. The Coulomb barriers for the emitted fragments are taken from empirical values in v3p, and calculated from the nuclear potential plus the Coulomb potential in ABLA07. ABLA07 also includes thermal expansion of the source.

4. In calculating particle-decay widths, ABLA07 includes the possibility of LCP tunnelling.

5. ABLA07 introduces an improved time-dependent decay width for fission, by utilising an approximated solution to the the Fokker-Planck equation [19], rather than the simple step function considered in v3p.

Note that the parameters in the ABLA07 code remain the same regardless of the system or incident energy being studied, and for this work their standard values, along with the standard values of the parameters in the INCL code, described in section 2.1, were used for all calculations. Also note, for reasons of brevity, the INCL4.2 plus ABLA version KHSv3p model will be referred to as INCL42 and the INCL4.5-ABLA07 model will be referred to as INCL45 for the remainder of this report.

3 Results and comparison with experimental data

3.1 Total reaction cross section

The total reaction cross section, used in calculating nucleon or LCP cross sections, was calculated using INCL42 and INCL45 for every reaction studied. Satisfactory agreement with experimental data was found in all cases and the two models differed in their calculations by less than 3% for nucleons incident on any target at $\geq$800 Mev, and by 11% or less for energies $<$800 MeV. Given the supposed deficiencies of INCL42 in predicting the total reaction cross section at low energies, these differences are suprisingly (although pleasantly so!) small. However, it should be pointed out that the apparently small difference between the two models actually represents a big advance in the way INCL4.5 calculates the total reaction cross section. In INCL4.2, the total reaction cross section calculation was done within the MCNPX package, which utilises some rather ad hoc parameters to improve predictions and prevent the dramatic underprediction seen in INCL4.2 otherwise. The results obtained using INCL4.5, however, were obtained independently of the MCNPX environment, benefiting instead from new physics introduced to the model to describe the Coulomb deflection of the incident projectile. Regardless of how it was calculated, due to the rather negligible difference in calculations of the total reaction cross section it was not thought to be responsible for any of the main differences between the two models. More in-depth studies of the total reaction cross section predicted by INCL42 and INCL45 have been previously conducted elsewhere, see for example [8] for more information.

3.2 Neutron cross sections

Figure 1 shows neutron double differential cross sections for proton induced reactions on Fe at 1200 and 800 MeV, as calculated by INCL42 (green lines) and

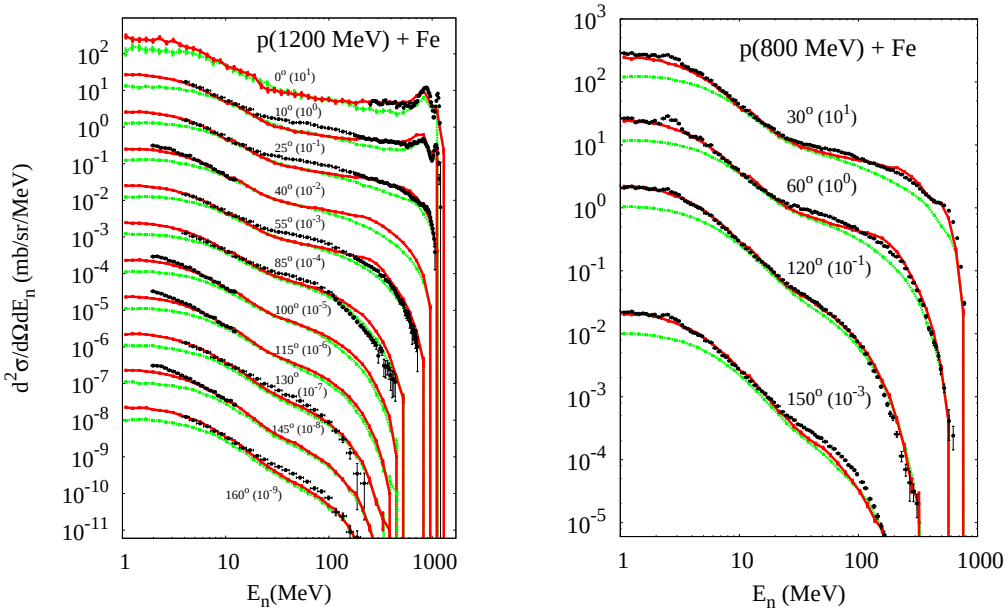

Figure 1: *Neutron double differential cross sections for proton induced reactions on an iron target with an incident energy of 1200 MeV (left) and 800 MeV (right). Predictions of INCL45 are given by red solid lines; predictions of INCL42 are given by green solid lines. The experimental data are given by solid circles and are taken from Refs. [20] and [21] for incident energies of 1200 and 800 MeV respectively. To ease the reading of the figure the data sets have been multiplied by decreasing powers of 10 with increasing angles, and these multiplying factors are given on the curves (in brackets) along with the values of the detection angles.*

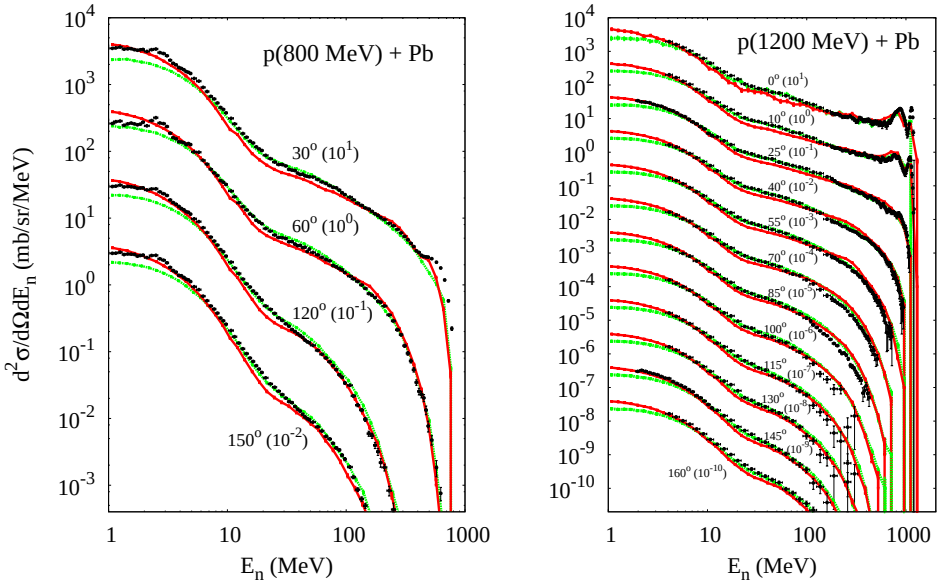

Figure 2: *Same as Figure 1, but for proton induced reactions on a lead target with an incident energy of 800 Mev (left) and 1200 MeV (right). The experimental data are taken from Refs. [21] and [20] for incident energies of 800 and 1200 MeV respectively.*

INCL45 (red lines). Figure 2 shows the same but for proton induced reactions on Pb at the same energies. The solid circles show experimental results for comparison. The simulations shown, along with all others carried out in this investigation, involved at least 2,000,000 events, in order to minimise the statistical uncertainties. As can be seen, both versions of the model show relatively good agreement with experimental data across the whole phase space, for both energies and target types. Both models adequately predict the quasi-inelastic peak (located at the beam energy minus ∼300 MeV for forward angles) at 1200 MeV for protons incident on both Fe and Pb, but INCL42 lacks any sort of high energy structure at 800 MeV. INCL45 triumphantly addresses this shortcoming, especially for Fe where the quasi-inelastic peak at around 500 MeV is excellently reproduced. The lack of calculated quasi-elastic peaks (located at around the beam energy for forward angles) in the calculations is down to the wide energy range studied for these simulations – which tends to mask thin features such as these – rather than a shortcoming of the models. For a better study of the performance of INCL42 around the quasi-elastic and inelastic peaks, see [5]. The only major shortcoming of either model is INCL42's systematic underprediction of the spectra in the evaporation regime, below around 20 MeV. Note similar results, not shown, were obtained with protons incident on Fe and Pb at 1600 and 3000 MeV, and also for Pb at 63 and 256 MeV. The same general level of agreement, along with the systematic low-energy underprediction by INCL42, was seen in all cases except for protons incident on Pb at energies less than 800 MeV, as will be discussed later.

It is not immediately clear which improvement in which code is responsible for INCL45's improvement of the low energy situation, due to the method by which neutron evaporation is calculated. The mean number of evaporated neutrons calculated by ABLA is taken, as mentioned in section 2.2, from the Weisskopf-Ewing model, by:

$$\langle n_{evap} \rangle \approx \frac{\overline{E^*}}{S_n + 2\bar{T}}, \tag{5}$$

where S_n is the mean neutron separation energy, E^* is the excitation energy left in the target after the cascade process and $\bar{T}$ is the mean temperature. Since, approximately, $\bar{T} = \sqrt{\overline{E^*}/a}$ [5], the number of evaporated neutrons really only depends on two variables, the excitation energy E^*, as calculated by INCL, and the so called level-density parameter, a, set in ABLA. The underprediction by INCL42 could thus be the result of either an incorrect prediction of E^* in INCL, or a poorly chosen value of a in ABLA. As it happens, the level density parameter was kept the same in both versions of ABLA, so only an improvement in the calculation of the excitation energy could be responsible for INCL45's improved calculation of $\langle n_{evap} \rangle$ from equation 5. A factor that can contribute to this improvement is INCL45's inclusion of an average potential for pions (see section 2.1). It is thought that the inclusion of a pion potential such as this decreases the number of pions emitted during the reaction, which in turn increases the number of evaporation neutrons [11]. Largely due to the (considerably) greater number of evaporation neutrons emitted in INCL45, the predicted total production cross sections of neutrons for proton on Fe reactions are around 20-30% higher in INCL45 than in INCL42. Outside the evaporation part of the spectra, the predictions of the two models are relatively similar, with the suggestion being that the main effect of the introduction of LCP emission is to slightly reduce the neutron spectra between about 20-100 MeV, although this is hardly a drastic change.

In the case of Fe, the new and expanded INCL45 performs slightly better, particularly at 800 MeV where the data is excellently reproduced at all angles over the entire energy range; the only exception to this being the small humps at around 2.5 MeV (the origins of which are unclear), which are not re-produced. INCL42, in contrast, tends to underpredict the spectra slightly, particularly at high energies. For proton on Pb reactions, however, INCL42 rather surprisingly outperforms INCL45, despite the latter's improved physics. This is particularly the case between around 10 and 100 MeV, where INCL45 underpredicts the spectra. This may be a result of the recent inclusion of an energy and isopsin dependent nuclear potential (see section 2.1), which has been found to reduce the cascade neutron multiplicity, whilst leaving the evaporation multiplicities essentially unchanged [10]. Interestingly, this reduction seems to be most prominent for Pb, as seen from our calculations. Another possibility is that this dip is the first sign of a quite serious problem with the new code when calculating proton on Pb reactions at low energies. As shown in Figure 3, at low energies the spectra do not exhibit minor dips, as we see in Figure 2, but huge, gaping chasms with minima at exactly 10 MeV, which dominate the calculated spectra. It is possible the slight dips at higher energy are early warning signs of the horrors that await one when plunging into the abyss of

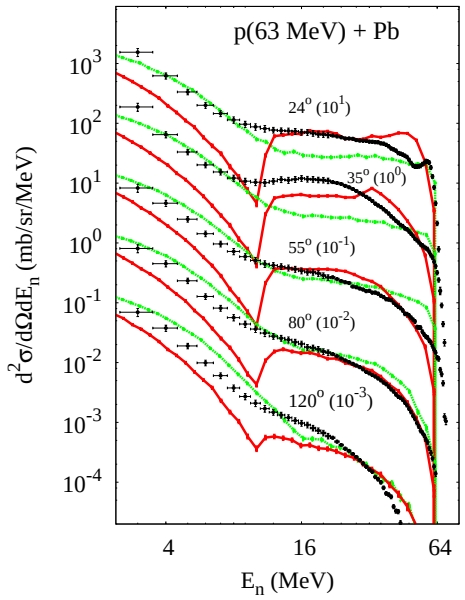

Figure 3: *Same as Figure 2 but at an incident energy of 63 MeV. The experimental data are taken from Ref. [22]. Note the minimum at exactly 10 MeV.*

INCL45's low energy proton on Pb predictions. This problem seems to have been introduced into INCL45 due a modification of the definition of so-called 'participants' and 'spectators'. Participant are defined as all deltas and pions, the incident nucleon, and any nucleons that have been involved in an avatar (as described in Section 2.1). The remaining nucleons are spectators. In INCL, only participants are considered as candidates for emission from the target. In INCL4.5, however, when the energy of a participant falls below some threshold value, set by a new parameter in the code, it is transformed back to a spectator, unable to be emitted. Therefore, no neutrons can be emitted at this threshold energy in the cascade regime. For the studies shown here, this parameter was set at 10 MeV, and as shown clearly in Figure 3 the mimimum is exactly at this value. Note that while nucleon emission is forbidden at this energy in the cascade model, evaporation nucleons are not affected by any such limitations, and it is due to this that the spectra valleys at 10 MeV become less prominent with increasing energy, since at higher energies there are more evaporation neucleons produced at the threshold energy, which compensate somewhat for the missing cascade nucleons. This shortcoming in INCL45 is an annoyance, to say the least, but work is currently undergoing in an attempt to eradicate this problem.

One further point should be discussed for neutron double differential cross-sections: as can be seen in Figure 1, it appears at first glance that INCL45 still underpredicts the spectra at low energies at 1200 MeV, despite a vast improvement over INCL42 and the fact that this is not seen at 800 MeV. Despite

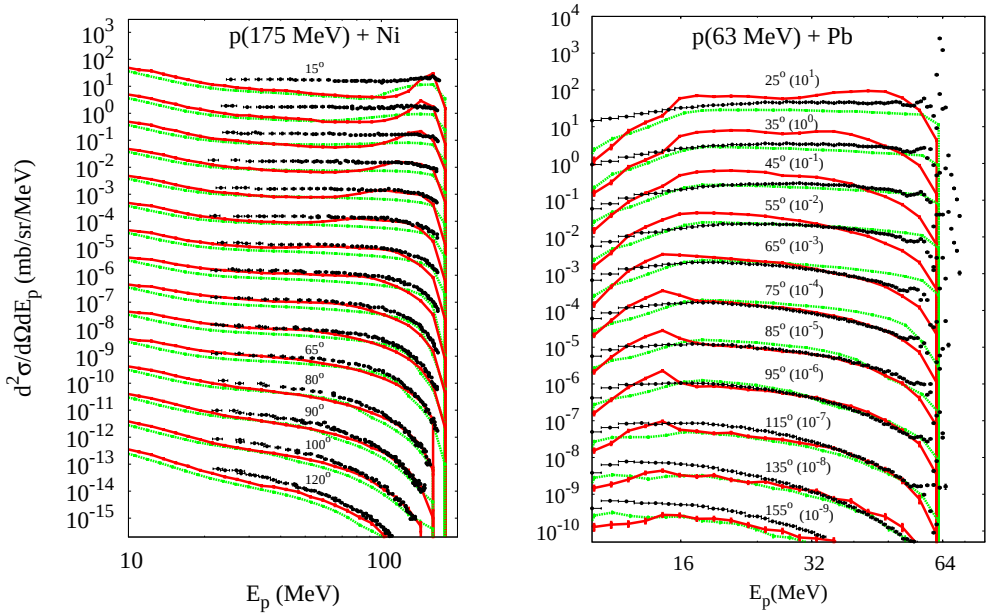

Figure 4: *Proton double differential cross sections for proton induced reactions on a nickel target at 175 MeV (left) and on a lead target at 63 MeV (right). Predictions of INCL45 are given by solid red lines; predictions of INCL42 are given by solid green lines. The experimental data are given by solid circles and are taken from Refs. [23] and [22] for Ni and Pb respectively. For Ni, the spectra are shown in* 5^o *steps from* 15^o *at the top of the figure, until* 65^o*, with the remaining angles labelled explicitly. To ease the reading of the figure the data sets have been multiplied by decreasing powers of* 10 *with increasing angles, starting at* 10^1 *for* 15^o*, up to* 10^{-13} *at* 120^o*. The detection angles and data multipliers are labelled explicitly for Pb.*

initial impressions, however, this is not due to a failing in the INCL45 model, but rather to the nuances in the experimental set-up used to obtain the data in each case. All the calculations presented in this paper, along with the data taken for Fe and Pb at 800 [21], assume or utilise a 'thin' target, whereas the data taken at 1200 MeV uses a 3cm Fe target and a 2cm Pb target [20]. In a thicker target, secondary reactions increase the number of low energy neutrons, accounting for the discrepancies seen whenever calculations are compared to [20]. Interestingly, as Figures 1 and 2 show, this effect seems to be more pronounced in the 3cm Fe target than the 2cm Pb one. See [20] for further discussion on the effects of target thickness on neutron spectra.

3.3 Proton cross sections

Figure 4 shows proton double differential cross sections for proton induced reactions on Ni at 175 MeV and Pb at 63 MeV, and Figure 5 the same for proton on Bi reactions at 62 MeV. Note that the yields are significantly lower than for

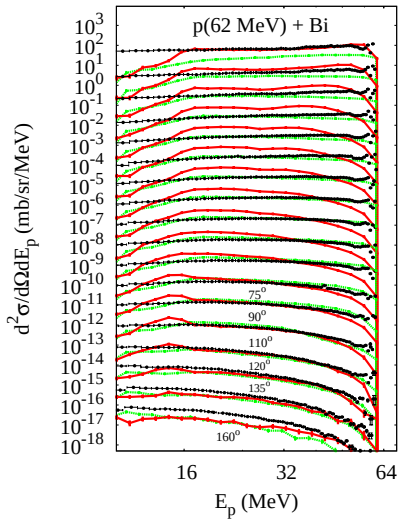

Figure 5: *Same as Figure 4 but for proton induced reactions on bismuth at 62 MeV. The experimental data are taken from Ref. [24]. The spectra are shown in* 5^o *steps from* 15^o *at the top of the figure up to* 75^o*, after which the angles are labelled explicitly. The data sets have been multiplied by decreasing powers of* 10*, from* 10^1 *at* 15^o*, up to* 10^{-16} *at* 160^o*.*

neutrons, showing that neutron emission is the dominant channel for particle production, as expected. It is immediately clear that the experimental spectra are not as well reproduced by the calculations as for neutrons, although the total production cross sections are fairly well reproduced (see [22] for example, which elucidates this for Pb at 63 MeV) in each case. The total production cross sections predicted by the two models differ by less than 7% for all reactions with incident energies of 800 MeV or higher. Not shown in Figures 4 and 5 is the low energy range below about 8-10 MeV, since the vast majority of protons are emitted in the cascade process and therefore results in this region, both experimental and theoretical, tend to be subject to large uncertainties that make it impossible to make meaningful comparisons here. Note similar calculations, not shown here, were carried out with protons incident on Fe at 62 MeV; Ta at 1200 MeV; Au at 1200 and 2500 MeV; and Pb at 800 MeV. Roughly the same level of agreement was seen for all reactions studied. In most cases both models seem to perform best at intermediate detection angles, between about 40^o and 90^o. INCL45 predicts slightly higher proton multiplicities in almost all cases, and this can be attributed to the introduction of a average pion potential and an energy and isospin dependent nuclear potential, as described in section 2.1. Both of these tend to increase the number of emitted protons, as discussed in Refs. [10] and [11]. On the whole, however, the predictions of the two models are fairly similar. The only exception to this is at low incident energies and forward angles, when INCL45 greatly overpredicts the spectra, while INCL42 is in excellent agreement with the experimental data, as shown in Figure 4 (right graph)

and Figure 5. At forward angles INCL45 even quite often predicts a strange, double-hump type structure that is not seen at all experimentally. This feature completely disappears for incident energies above 63 MeV and its existence is clearly indicative of a problem that needs to be addressed. The lower energy hump is probably a consequence of the particle/spectator modifications mentioned in section 3.2 (since it is only prominent at low incident energies), and once that problem is solved it will likely disappear. The higher energy hump may be a consequence of difficulties in calculating the location and magnitude of the quasi-elastic peak, and may be more difficult to remove.

It is worth bearing in mind, however, the validity of the INC approach for reactions with incident energies as low as this. Due to the nature of the INC model (as described in section 2.1), it should really only be applicable in the (classical) independent collision regime, i.e. when:

$$\lambda_B << r_s < d, \tag{6}$$

where λ_B is the de Broglie wavelength, r_s is the range of the nuclear forces and d is the average distance between neighbouring nucleons [8]. This condition is only satisfied for incident energies above 200 MeV *at best*. Given the plethora of quantum effects that are expected to come into play for incident energies as low as 63 MeV, the fact that any kind of agreement with experiment is seen appears to be, at first glance, nothing short of miraculous. However, the agreement that is seen, which can be quite good in some cases, does in fact have several plausible explanations (see [25] for further discussion of this point).

3.4 Helium-4 cross sections

Figure 6 shows helium-4 double differential cross sections for proton induced reactions on Au at 1200 MeV and Fe and 62 MeV, and Figure 7 shows the same for proton induced reactions on Au at 2500 MeV. Before looking at these results in too much detail, it is worth mentioning that, as originally stated in sections 2.1 and 2.2, ^{4}He production in INCL42 is only considered in the evaporation regime, which accounts for the swift drop off in the spectra after around 20 MeV. Due to this shortcoming in INCL42 the total production cross sections for ^{4}He predicted by the two models differed wildly in most cases, making a meaningful comparison between the two models impossible.

Of the possible LCP that can be emitted in INCL45, only ^{4}He has been considered in this study. Other LCP production within INCL45, i.e. tritium, helium-3 and deuteron, has recently been examined elsewhere [28], where it was found that the model shows good agreement with experimental data in most cases, especially at higher incident energies. ^{4}He production was found to be the most accurately predicted LCP (protons excluded), however, and also the LCP for which the cascade contribution is the smallest. It is due to this, and the fact that INCL42 can only consider LCP production in the evaporation part of the spectrum, that we have restricted this investigation to ^{4}He cross section calculations. As the higher energy parts of Figures 6 and 7 show, LCP production modelling in INCL45 has clearly been a success, seeing excellent agreement with the data, and the angle and energy dependence of the spectra well reproduced on the whole. Studies were also carried out for protons incident

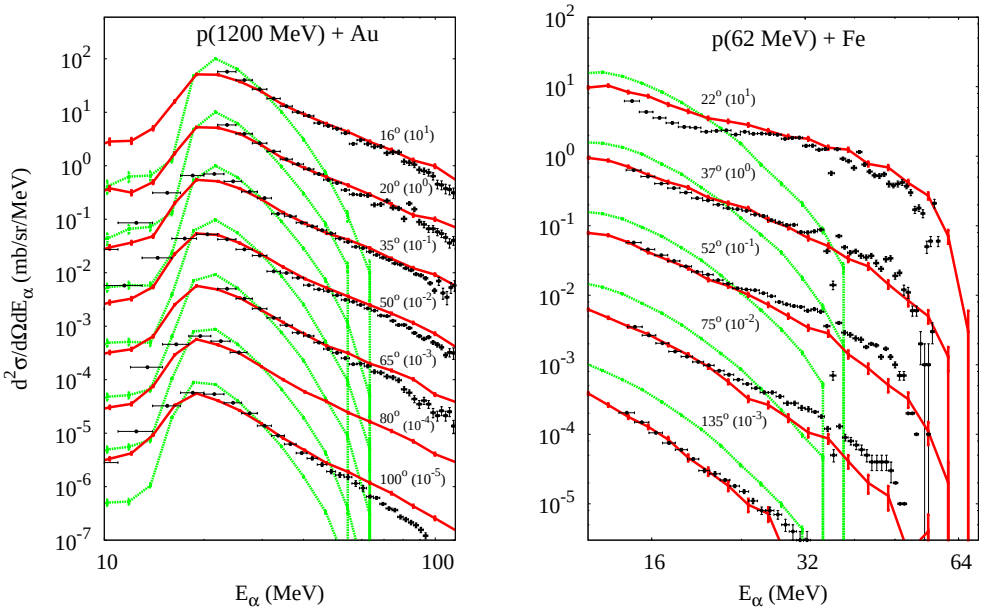

Figure 6: ^{4}*He double differential cross sections for proton induced reactions on a gold target at 1200 MeV (left) and on an iron target at 62 MeV (right). Predictions of INCL45 are given by solid red lines; predictions of INCL42 are given by solid green lines. The experimental data are given by solid circles and are taken from Refs. [26] and [24] for Au and Fe respectively. To ease the reading of the figure the data sets have been multiplied by decreasing powers of 10 with increasing angles, and these multiplying factors are given on the curves (in brackets) along with the values of the detection angles.*

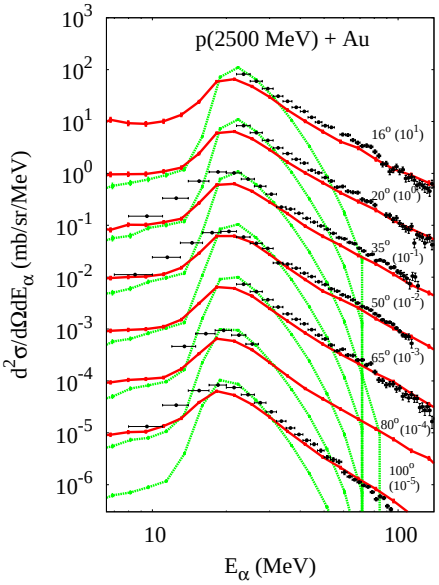

Figure 7: *Same as Figure 6 but for proton induced reations on a gold target with an incident energy of 2500 MeV. The experimental data are taken from Ref.[27].*

on: Bi at 62 MeV; Al at 160 MeV; Ta at 1200 MeV; Au at 160 MeV; and Pb at 63 MeV, with the INCL45 calculations showing similar agreement with the experimental data each time, and INCL42 suffering from the same high energy shortcoming each time. Of particular interest in the calculations is the behaviour of the two models in the evaporation regime, since both versions v3p and 07 of ABLA can accomodate ^{4}He production. Clearly INCL45 is superior in the low energy range, with INCL42 underpredicting the spectra by anything up to an order of magniture below about 15 MeV. Whilst this improvement may be due in part to the inclusion of LCP production in INCL4.5, ABLA07 has been modified from v3p to allow the possibilty of LCP tunnelling when calculating particle-decay widths, and this may also be able to take some of the credit.

Careful inspection of the Figures 6 and 7 reveals that there is at least one area, however small, where INCL45 does not completely outstrip its older incarnation: the peaks in the spectra between 10-20 MeV. INCL45 has a tendancy, for nearly all the reactions studied, to underpredict the very top of the peaks, whereas the height of INCL42's peaks are in good agreement with the data, even if the spectra shapes are dramatically wrong. Given the much too steep sides of the spectra mountains predicted by INCL42, this is not particularly significant, but of more interest is the performance of an interim INCL-ABLA version, INCL4.3 + v3p (henceforth called INCL43), in similar cicumstances. INCL4.3 was the first to include all LCP production (at least in the cascade regime), and, as shown in [29], it also predicts the height of the peaks better. However, unlike INCL42, this version also manages to predict the high energy

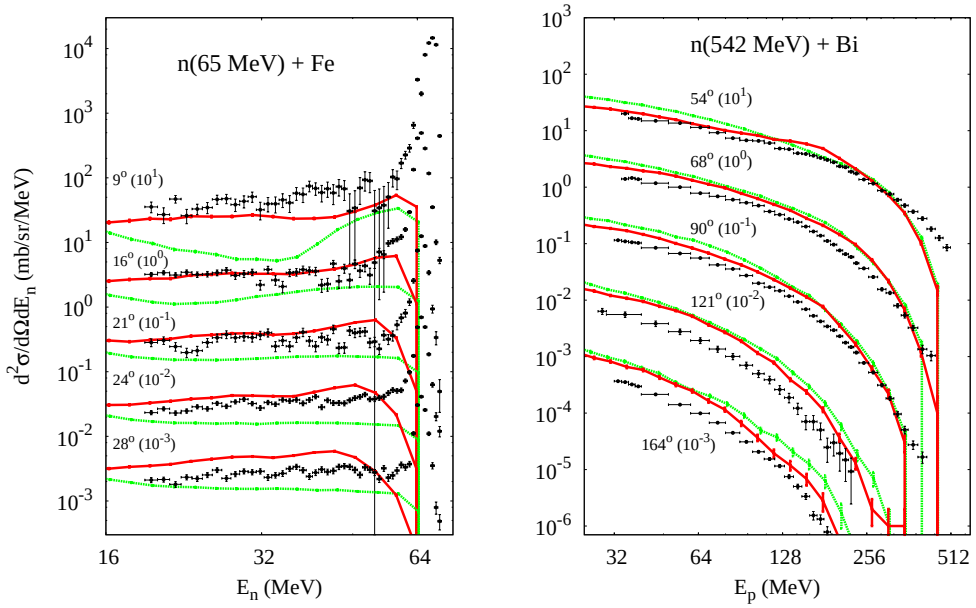

Figure 8: *Neutron double differential cross sections for neutron induced reactions on a Fe target at 65 MeV (left) and proton double differential cross sections for neutron induced reactions on a Bi target at 542 MeV (right). Predictions of INCL45 are given by solid red lines; predictions of INCL42 are given by solid green lines. The experimental data are given by solid circles and are taken from Refs.[30] and [31] for Fe and Bi respectively. The detection angles and multiplying factors are labelled on the graphs, as in previous figures.*

tail of these spectra much more accurately (although not quite as accurately as INCL45). Although small differences [8] in the ways clusters are emitted in INCL4.3 and INCL4.5 may have some impact on the peak heights, other work [28] has shown the biggest contribution to the height of the peaks in ^{4}He spectra comes from the evaporation model used. ABLA07 can cater for LCP and IMF emission in addition to the nucleon and ^{4}He emission included in v3p, and this likely explains the differences seen. Any ^{4}He particles under consideration for emission in the evaporation region in INCL45 will face increased competition, not just with nucleons, as before, but with a wide range of emission candidates, all jostling for selection. Therefore, they will slightly less likely to be emitted, accounting for the discrepancy between the two versions. Thus, improved modelling of, for example, deuteron and proton double differential cross sections, as seen in [7], may have come at a price: reduced ablity to accurately predict the peak heights in the ^{4}He and ^{3}He spectra.

3.5 Neutrons as incident particles

Two reactions with neutrons as the incident particles were also studied. First, neutrons on Fe at 65 MeV, with neutron double differential cross sections calcu-

lated; Second, neutrons on Bi at 542 MeV, with proton double differential cross sections calculated. The results are presented in Figure 8. Low energy predictions are not shown due to the lack of experimental data in this region (and for neutrons on Bi most protons are emitted in the cascade process anyway). The large quasi-elastic peak at forwards angles for neutrons on Fe is probably not predicted due, in part at least, to the (relatively) large size of the energy bins used in the calculation, rather than a major shortcoming of the model. Given that only two reactions with incident neutrons were studied, and that for those two different observables were calculated, it would be imprudent to draw too many conclusions from the results obtained. We can at least say, however, that for both reactions studied INCL45 gives better results, and, sometimes (for example with neutrons incident on Fe very forward angles), *much* better results. In theory the nature of the projectile used in a calculation (neutron or proton) should be of little consequence to the result, but clearly more calculations and experiments need to be carried out to establish more comprehensively the effects of the recent modifications on the predictions of observables from neutron induced reactions.

4 Conclusion

New and old versions of the INCL-ABLA model for studying spallation reactions have been compared by considering their prediction of a number of observables for nucleons incident on a large selection of targets at a wide range of incident energies. Calculations using the earlier version of the model were performed in MCNPX using the default parameters at all times, while the predictions of the new model were taken from the IAEA 'Benchmark of Spallation Models' project, along with the experimental data – used to aid comparison of the two models. It was found that key improvements, particularly the introduction of LCP emission in the new version, have caused great strides to be made in some predictions, particularly those of ^{4}He production cross-sections. Predictions of neutron production out of proton on Fe reactions have also been significantly improved across the entire energy range; however, similar prediction for proton on Pb are not as impressive and are in fact totally dominated by a spurious artifact (whose origin has been identified). Predictions of proton production cross sections are also something of a mixed bag, with great improvements seen in some areas, but problems, most often overpredictions, seen in others. The overall trend is towards improvement, however, and it is hoped that further research will rid the model of these relatively minor, but nonetheless irritating deficiencies in the near future.

ACKNOWLEDGMENTS

- Bijan Saghai, for giving me the opportunity to work with him and on this project.
- Jean-Christophe David, for suggesting the project and the time he spent pointing me in the right directions.
- Alain Boudard and Jean-Christophe David, for their careful proof-reading of this report and many helpful comments.

References

[1] C.D.Bowman, E.D. Arthur, P.W.Lisowski *et al*, Nucl. Instrum. Meth. A **320**, 336–67 (1992).

[2] I.Tanihata, *Treatise on Heavy-Ion Science*, edited by D.A.Bromley (Plenum Press, New York, 1989), Vol.8.

[3] R.Silberberg and C.H.Tsao, Phys. Rep. **6**, 351–408 (1990).

[4] S.Leray, A.Boudard, J.Cugnon *et al*, Nucl. Instrum. Meth. A **562**, 806–9 (2006).

[5] A.Boudard, J.Cugnon, S.Leray and C.Volant, Phys. Rev. C **66**, 0044615 (2002).

[6] H.Ullmaier and F. Carsughi, Nucl. Instrum. Meth. B **101**, 406–21 (1995).

[7] http://www.nds.iaea.org/spallations.

[8] A.Boudard and J.Cugnon, in: D.Filges, S.Leray, Y.Yariv, A.Mengoni, A.Stanculescu and G.Mank (Eds.), *Proceedings of the Joint ICTP-IAEA Advanced Workshop on Model Codes for Spallation Reactions*, ICTP Trieste, Italy, February 4–8, 2008, IAEA INDC(NDS)-530, Vienna, August 2008, p29. Availiable from: <http://www-nds.iaea.org/reports-new/indc-reports/indc-nds/ indc-nds-0530.pdf>.

[9] R.Woods and D.Saxon, Physical Review **95** (2), 577–8 (1954).

[10] Th.Aoust and J.Cugnon, Eur. Phys. J A **21** 79–85 (2004).

[11] Th.Aoust and J.Cugnon, Phys. Rev. C **74** 064607 (2006).

[12] A.Kelic, M.V.Ricciardi and K.-H.Schmidt, in: D.Filges, S.Leray, Y.Yariv, A.Mengoni, A.Stanculescu and G.Mank (Eds.), *Proceedings of the Joint ICTP-IAEA Advanced Workshop on Model Codes for Spallation Reactions*, ICTP Trieste, Italy, February 4–8, 2008, IAEA INDC(NDS)-530, Vienna, August 2008, p.181. Availiable from: <http://www-nds.iaea.org/reports-new/indc-reports/indc-nds/ indc-nds-0530.pdf>.

[13] V.F.Weisskopf and D.H.Ewing, Phys. Rev. **57**, 472–85 (1940).

[14] J.Benlliure, A.Grewe, M.de Jong, K.-H.Schmidt and S.Zhandov, Nucl. Phys. A **14**, 458–78 (1998).

[15] K.-H.Schmidt, A.Kelic and M.V.Ricciardi, Eur. Phys. Lett. **83** 32001 (2008).

[16] K.-H.Schmidt, M.V.Ricciardi, A.Botvina and T.Enqvist, Nucl. Phys. A **710**, 157–79 (2002).

[17] A.R.Junghans, M.de Jong, H.G.Clerc, A.V.Ignatyuk, G.A.Kudyaev and K.-H.Schmidt, Nucl. Phys, A **629**, 635–55 (1998).

[18] J.-J.Gaimard and K.-H.Schmidt, Nucl. Phys. A **531**, 709–45 (1991).

[19] B.Jurado, C.Schmitt, K.-H.Schmidt, J.Benlliure and A.R.Junghans, Nucl. Phys. A **757** 14–43 and 329–348 (2005).

[20] S.Leray, F.Borne, S.Crespin *et al*, Phys. Rev. C **65** 044621 (2002).

[21] W.B.Amian, R.C.Byrd, C.A.Goulding, G.L.Morgan, C.E.Moss and D.A.Clark, Nucl. Sci. Eng. **112** 78–86 (1992).

[22] A.Guertin, N.Marie, S.Auduc *et al*, Eur. Phys. J. A **23** 49–60 (2005).

[23] S.V.Foertsch, A.A.Cowley, J.J.Lawrie, D.M.Whittal, J.V.Pilcher and F.D.Smit, Phys. Rev. C **43** 691–700 (1991).

[24] F.E.Bertrand and R.W.Peelle, Phys. Rev. C **8** 1045–64 (1973).

[25] Y.Yariv, T.Aoust, A.Boudard, J.Cugnon, J.C.David, S.Lemaire and S.Leray, *Proceedings of the International Conference on Nuclear Data for Science and Technology* 1125–8 (2008).

[26] A.Budzanowski, M.Fidelus, D.Filges *et al*, Phys. Rev. C **78** 024603 (2008).

[27] A.Bubak, A.Budzanowski, D.Filges, *et al*, Phys. Rev. C **76** 014618 (2007).

[28] S.Leray, A.Boudard, J.Cugnon, J.C.David, A.Kelic-Heil, D.Mancusi and M.V.Ricciardi, Nucl. Instrum. Meth. B **268** 581–6 (2010).

[29] A.Boudard, J.Cugnon, S.Leray and C.Volant, Nucl. Phys. A **740** 195–210 (2004).

[30] E.L.Hjort, F.P.Brady, J.R.Drummond *et al*, Phys. Rev. C **53** 237–42 (1996).

[31] J.Franz, P.Koncz, E.Roessle *et al*, Nucl. Phys. A **510** 774–802 (1990).